Applications of microbeam analytical techniques in gold deportment studies and characterization of losses during the gold recovery process

Stamen S. Dimov* [iD] and Brian R. Hart

Many gold deposits are characterized by the presence of refractory (submicroscopic) gold in the matrix of sulfide minerals which is not directly amenable to gold cyanidation. In order to recover this submicroscopic gold, the ore has to be oxidized before being subjected to gold cyanidation and extraction. This is done by autoclave pressure oxidation (AC POX), a technology commonly used in the mining industry for ores with a high refractory gold content. Gold ores commonly contain active carbonaceous materials which have the ability to adsorb, or preg-rob, gold during the AC POX and/or cyanidation steps of the recovery process, and gold losses can be significant.

Advanced microbeam analytical techniques such as dynamic secondary ion mass spectrometry (D-SIMS) and time-of-flight secondary ion mass spectrometry (TOF-SIMS) have become powerful tools for characterization of different forms and carriers of gold in the mining industry. Major advantages of these techniques are related to the investigation of individual mineral particles and quantitative analysis with detection limits in the low ppm/ppb concentrations. This paper describes various microbeam techniques and procedures implemented at Surface Science Western (SSW) which have become an intricate part of a comprehensive mineralogical and analytical approach for ore characterization and process mineralogy. Copyright © 2017 John Wiley & Sons, Ltd.

Keywords: gold recovery; gold deportment; refractory gold; carbonaceous matter; preg-robbing; dynamic SIMS; TOF-SIMS

Introduction

Accurate, detailed information about the gold content and distribution within a feed ore sample or process stream product is of crucial importance for identifying potential losses and optimizing the gold recovery process. The implementation of advanced microbeam analytical techniques such as dynamic secondary ion mass spectrometry (D-SIMS)[1–3], time-of-flight secondary ion mass spectrometry (TOF-SIMS),[4,5] and time-of-flight resonance ionization mass spectrometry (TOF-RIMS)[6] in the mineral industry has resulted in the development of comprehensive protocols to accurately identify and assess the carriers and forms of gold in mineral samples. Major advantages of these techniques are related to their ability to directly analyze individual mineral particles, provide quantitative analysis with detection limits in the low ppm/ppb concentration range, and image the gold distribution within the host minerals.

Autoclave pressure oxidation (AC POX) of refractory sulfide ores and subsequent cyanidation is a common technology used to recover the submicroscopic gold in these types of ores. A major obstacle for effective gold recovery during this process is the presence in the ores of active carbonaceous matter (C-matter) which has the ability to adsorb, or preg-rob, gold from the cyanide leach solution.[7–9] Therefore, it is important to develop technology and procedures for (1) evaluation of the preg-robbing capacity and (2) direct quantitative determination of the surface gold preg-robbed on the C-matter. Surface microbeam analytical techniques such as time of flight laser ionization mass spectrometry (TOF-LIMS) and

time of flight secondary ion mass spectrometry (TOF-SIMS) were first introduced for characterization of sorbed gold species on c-matter from CIL tails samples by Dimov et al.[4,5] Recent development and introduction of a new generation of cluster liquid metal ion sources (Bi^{3+} and Au^{3+}) to the TOF-SIMS instrumentation have led to a dramatic improvement of the detection sensitivities and ability to identify complex compounds with minimum molecular fragmentation. The TOF-SIMS technology provides non-destructive elemental and molecular surface analysis and allows for simultaneous detection and imaging of the distribution of surface metallic gold and gold compounds on individual carbonaceous particles. The quantification of the TOF-SIMS data is based on element and compound specific standards with established detection limits for surface metallic and compound gold in the low ppm range.[2,5]

* *Correspondence to: Stamen S. Dimov, Surface Science Western, Western University, 999 Collip Circle, London, ON N6A 5B7, Canada.*
E-mail: sdimov@uwo.ca

Surface Science Western, Western University, 999 Collip Circle, London, Ontario, N6A 5B7, Canada

Characterization of carbonaceous matter in terms of preg-robbing properties

While it is now possible to quantitatively evaluate and speciate the surface gold preg-robbed on carbonaceous matter from process stream products, it is equally important to develop predictive tools for characterization and assessment of the preg-robbing behavior of C-matter in an ore sample. The capacity of C-matter to preg-rob may vary between ores as well as within a single ore body. Currently, there is no single parameter which can be used to fully describe the preg-robbing capacity of an ore. Thus, plant operations are continuously challenged by this highly variable and significant characteristic.

Recognizing the importance and the effect of gold preg-robbing on C-matter during the gold recovery process, an analytical protocol has been developed for the characterization of C-matter and its preg-robbing properties.[7] The procedure utilizes a set of complementary microbeam analytical techniques (scanning electron microscopy coupled with energy dispersive x-ray analysis: SEM/EDX, laser Raman spectroscopy) along with surface area measurements (BET) and standardized doping tests. These techniques can provide information on many of the variables affecting the preg-robbing properties of the C-matter, including its composition, maturity, and surface area that can be used as a predictive tool. Normalized preg-robbing indices are introduced which can accurately describe the preg-robbing capacity of C-matter across a set of samples and allow for comparative analysis between different ores or between composite samples within the same ore body. The data library on preg-robbing capacities of C-matter from a large number of commercial mines generated to date shows a very large dynamic range with differences in maximum preg-robbing capacity up to 200 times.[7] A comparative analysis of the data indicates that, along with the total organic carbon (TOC) content and exposed surface area (as defined by BET analysis), the maturity or the degree of disorder of the naturally occurring C-matter within the ore has been linked to its pre-robbing capacity.[9]

Compositional and morphological analysis of carbonaceous material: SEM/EDX study

SEM/EDX is an effective tool for evaluating the morphology and distribution of various types of C-matter. Moreover, the samples can be examined in both cross section and as grain mounts. The latter provides information regarding surface coatings or can identify fragments of carbon on the surface of gangue grains.

Two different types of C-matter are usually identified in the carbonaceous ore samples:

- Total C-matter (TCM) particles defined as particles that consist of >80% C-matter (Figure 1). They may contain very small inclusions or surface attached gangue particles as is indicated by the presence of elements such as Al, Si, S, Ca, and/or Fe in their EDX spectra and the SEM images.
- Disseminated C-matter (DCM) particles. These are defined as compositionally variable particles (ie, quartz or other gangue minerals) with different degrees of finely DCM (see Figure 2). The distribution of the C-matter on these particles is patchy and shows high variability among grains and ores.

Backscattered electron images (BSE) of DCM particles from a feed ore are shown in Figure 2. EDX analysis of the dark areas on the

	C	O	Al	Si	S	Fe
TCM-1	73.5	19.3	0.4	2.4	1.2	3.2
TCM-2	85.1	13.7			1.1	
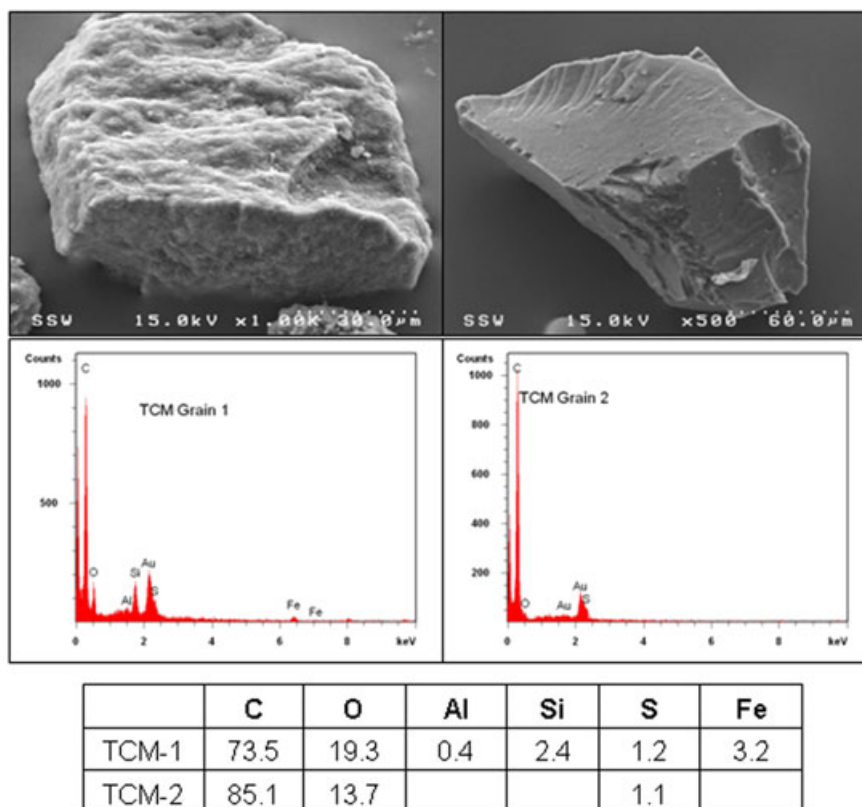
Figure 1. Secondary electron images (SEI), EDX spectra, and semiquantitative elemental analyses of selected areas on 2 TCM grains from an ore sample. All data are in wt.%. Note: samples were Au coated for imaging purposes

	C	O	Mg	Al	Si	S	K
CILF Gr 17 SP1	85.4	10.0		0.3	0.4	3.6	
CILF Gr 17 SP2	85.1	52.1	0.6	4.1	41.2		2.0
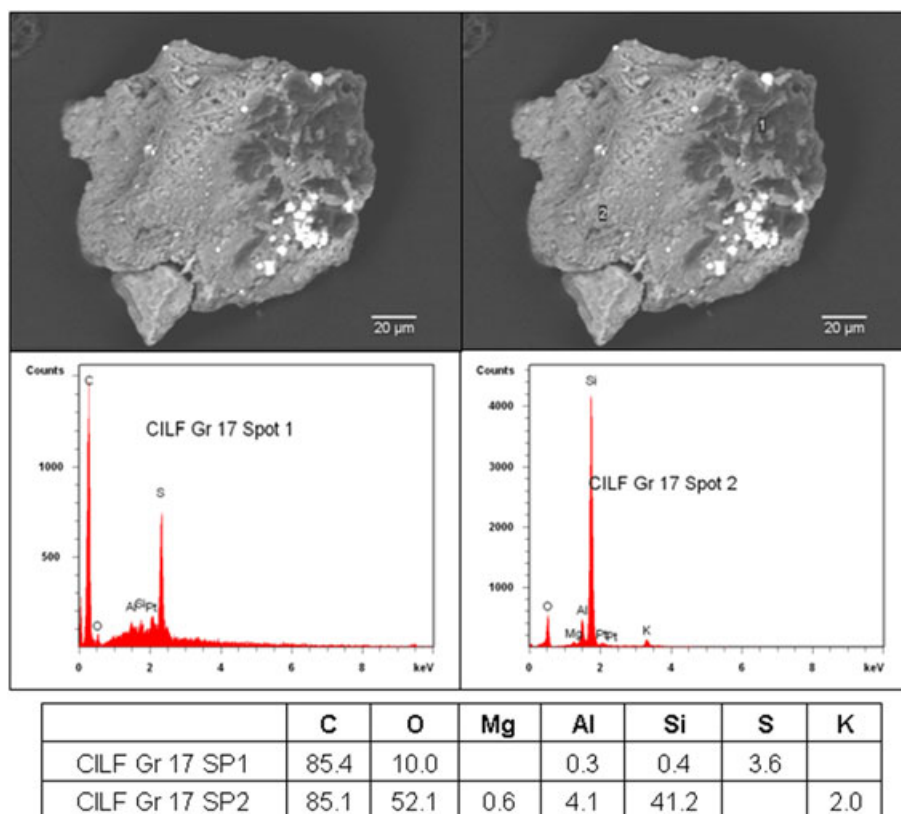
Figure 2. Back scattered electron images (BSE), EDX spectra, and semiquantitative elemental analyses of selected regions on a DCM grain from an ore sample. The numbers in the images refer to the areas analyses and correspond to the spectra and data in the table. All data are in wt.%. Note: samples were Pt coated for imaging purposes

grains indicates compositions dominated by C, whereas the lighter regions contain variable proportions of Si, Al, and O.

Structural characterization of the C-matter by laser Raman spectroscopy

The preg-robbing capacity of C-matter can be correlated to the degree of C organization (order). Graphite, which is highly ordered, shows very poor preg-robbing characteristics, whereas activated carbon, which is highly disordered, shows strong preg-robbing characteristics.

Raman analysis can be used as a diagnostic tool capable of predicting and differentiating the preg-robbing properties of C-matter.[7,9] For such a study, a comparative analysis is conducted on the intensity, bandwidth, and frequency shifts of the D and G bands for carbonaceous particles from ore samples and from reference samples of graphite and activated carbon (examples of each are given in Figure 3). The figure also shows the deconvolution peak fits used for the maturity classification procedure. Examples of SEM images along with Raman spectra for selected grains containing C-matter are given in Figures 4 and 5.

In order to comparatively evaluate and present the degree of disorder of the C-matter in each sample, the Raman ratio, which reflects the measured degree of disorder in the carbon structure and its potential for preg-robbing, is calculated and displayed on a scatter plot (see Figures 6 and 7). The ratio is calculated from the deconvoluted Raman spectra. Literature and research evaluations have shown that the preg-robbing capacity of the carbonaceous matter is positively correlated with increasing degree of disorder.[9]

### Standardized doping tests/maximum preg-robbing capacity/preg-robbing indices

An evaluation of the maximum preg-robbing capacity of samples containing carbonaceous matter is done through doping tests using controlled amounts of $Au(CN)_2$ in solution. The amount of preg-robbed surface gold in these doped samples is determined as a difference between the Au assayed values in as-received and doped samples for each corresponding sample. The determined maximum preg-robbing capacity of the C-matter from doping tests provides an important insight on the expected behavior of this ore during the process of gold recovery. The degree of preg-robbing is governed by several different parameters:

- Total organic carbon: the TOC content in the sample is assayed using a standard Leco analytical procedure.
- Surface area: the "exposed" total surface area of the C-matter particles is determined by Brunauer-Emmett-Teller (BET) surface area analysis.
- Nature (maturity/disorder) of the C-matter.
- The presence of various functional groups on the surface of the C-matter (ie, the surface chemistry of the C-matter) that may have an additional effect on its preg-robbing capacity

Standardized doping tests provide an estimate on the maximum preg-robbing capacity. A comparative analysis between the established values for maximum preg-robbing capacities, TOC content, and the Raman ratio data on the degree of disorder in the carbon structure is shown in Figure 7 (upper). The data show that there is a fairly good correlation between decreasing order and increasing preg-robbing capacity. In this particular deposit, the highest degree
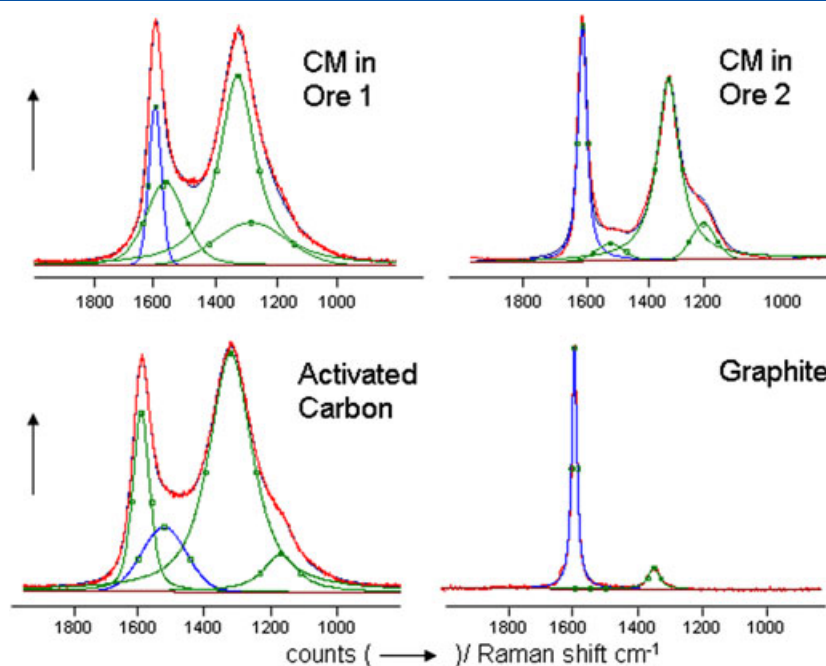
Figure 3. Examples of Raman spectra from C-matter identified in carbonaceous ores, and spectra from activated carbon and graphite along with peak fits used to identify the degree of C disorder in C-matter and discriminate different carbonaceous species
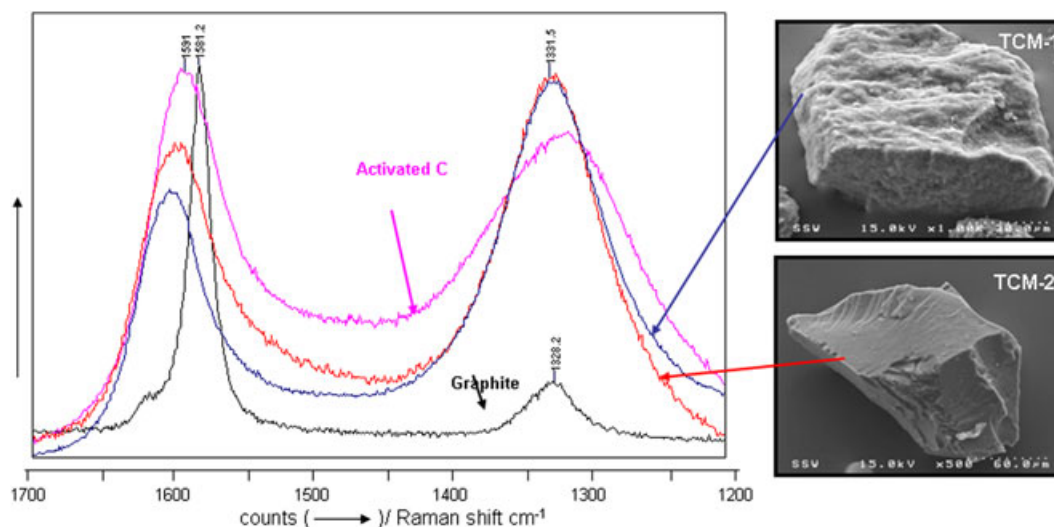

Figure 4. Secondary electron images and Raman spectra from 2 carbonaceous (TCM) grains. Also included are reference Raman spectra from graphitic carbon and activated carbon

of disorder for the C-matter is seen in ore 3 which also shows the highest preg-robbing capacity. It should be emphasized that ore 3 has on the order of 2× the TOC relative to all other samples in the ore, but its preg-robbing capacity is in the order of 4× any other sample. A second feature noted from this data is that the preg-robbing capacity of ore samples 2 and 4 correlates very well to their TOC content; ore 4 is approximately 2× greater in TOC and shows 2× the preg-robbing capacity. The Raman ratio for both ores spans the same region suggesting that the C-organization of the TOC in these samples is similar and that the preg-robbing is more related to the proportion and distribution of the C-matter.

Normalized preg-robbing indices are introduced that describe the preg-robbing capacity of C-matter across a set of samples and allow for comparative analysis between different ores or between composite samples within the same ore body.[7] In order to establish a more objective preg-robbing index for the C-matter, the raw data from the preg-robbing tests are normalized by the BET surface area assayed for the studied samples. Assays for TOC evaluate the proportion of carbon within the sample regardless of the TOC surface properties/accessibilities that are associated with its capacity to preg-rob. Depending on the composition and the distribution of the C-matter, much of the assayed carbon may not be available for preg-robbing and likely resides within grains that are not accessible to leachate. The BET analysis, on the other hand, reflects the surface adsorption capacity of the material and, as such, provides a much better estimate of the effective surface area available for leachate interaction and potential preg-robbing.
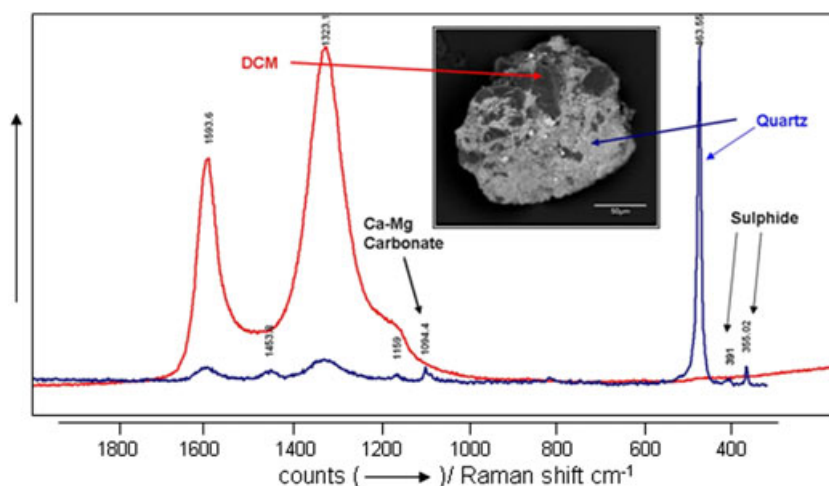
Figure 5. Backscattered electron image of a disseminated carbonaceous matter (DCM) particle from an ore sample along with Raman spectra from 2 different regions representing carbonaceous matter and the gangue mineral
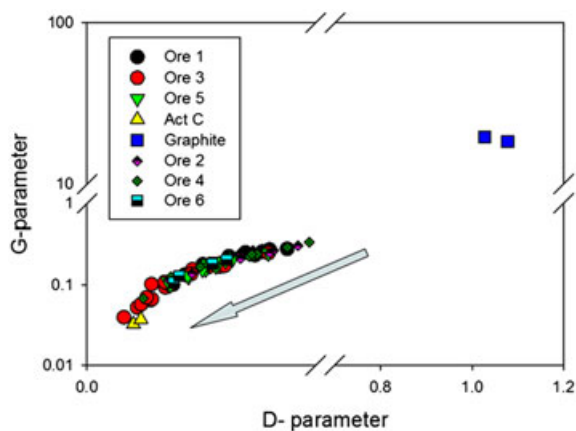
Figure 6. Raman ratio plot for activated carbon and graphite along with several ores within a single deposit. The data illustrate the variability of the inherent C structural order for the various zones within the ore. The arrow illustrates the general trend of increasing preg-robbing capacity

Preg-robbing indices, based on normalization by the BET, more accurately represent the preg-robbing characteristics of C-matter across the set of samples analyzed and provide a more objective basis for comparison. The data shown in Figure 8 clearly illustrates that MPRC normalized to TOC has a tendency to overestimate the samples preg-robbing capacity, whereas when normalized to BET the estimation is more reflective of the actual capacity of the sample to adsorb the lixiviant.

Gold deportment studies

Definition of gold deportment studies

The extractive metallurgy of gold is largely driven by the mineralogical association of the Au and the composition of the ore. Factors that influence extraction efficiency include liberation, particle size, mineral association, surface coatings, presence of cyanicides, oxygen consumers, preg-robbers, presence of refractory gold minerals, and locking of submicroscopic gold in sulfide mineral structures.

The scope of a full deportment study is to establish all forms and carriers of gold present in the ore sample.[1–3,10,11] Forms of gold refer to microscopic (visible) gold, submicroscopic (invisible or refractory) gold, soluble gold salts, and surface bound gold. Carriers of gold refer to all major host materials carrying 1 or more of the abovementioned forms of gold. Accurate, detailed information about the forms and carriers of gold in a feed or process stream sample is of crucial importance for optimization of the gold recovery process and identifying potential losses.

The full gold deportment study is based on a comprehensive mineralogical and analytical procedure. It includes assays, optical microscopy, and a set of microbeam analytical techniques which provide independent quantitative estimates and characterization of different forms of gold in a variety of carriers. Based on these data, a gold deportment balance/diagram is established which addresses all forms and carriers of gold present in the sample.

The evaluation process includes the following:

- Assays
- QEMSCAN modal and XRD analysis
- High spatial resolution SEM/EDX scans for visible gold phases
- Identification and quantitative analysis of carriers of submicroscopic gold among the relevant mineral phases present in the samples by dynamic SIMS (D-SIMS).
- Quantification and speciation of preg-robbed surface gold on C-matter by D-SIMS and TOF-SIMS

Microbeam techniques used for characterization of various forms/carriers of gold

Characterization of visible gold

The visible gold is characterized using high-resolution visible gold scans produced by a field emission SEM-EDX instrument (model Hitachi 6600 VP-FEG-SEM). The magnification used allows detecting and characterizing visible gold particles with dimension down to 1 to 2 microns. Detailed visible gold SEM/EDX scans on polished sections prepared from super-panned fractions of samples provide
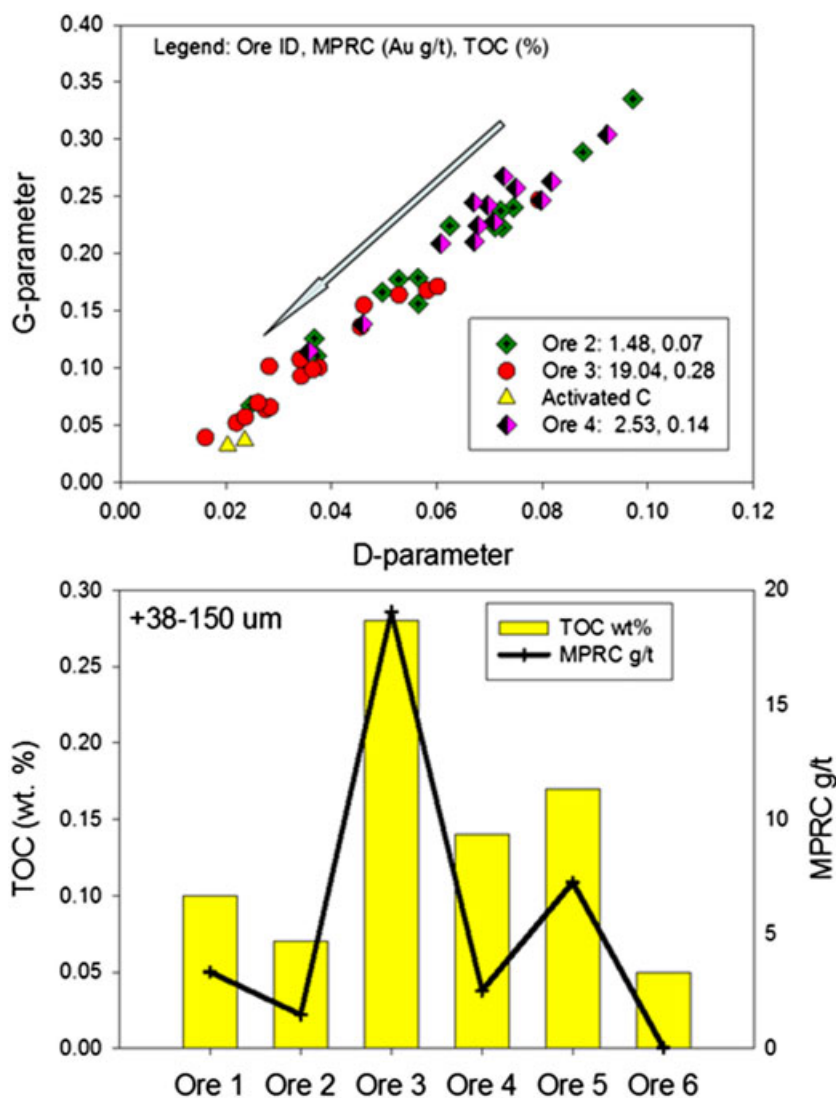
Figure 7. Upper: Raman ratio plot for activated carbon and 3 different ore zones within a single deposit. Also shown on the figure for each ore are the maximum preg-robbing capacity, MPRC (Au, g/t), and TOC (total organic content). The arrow shows the increasing trend of preg-robbing capacity. Lower: Total organic carbon content (TOC) and maximum preg-robbing capacity for 6 ore zones within a single deposit. Note: ores 2, 3, and 4 (identified by red stars) are the same ores as shown in the upper Figure
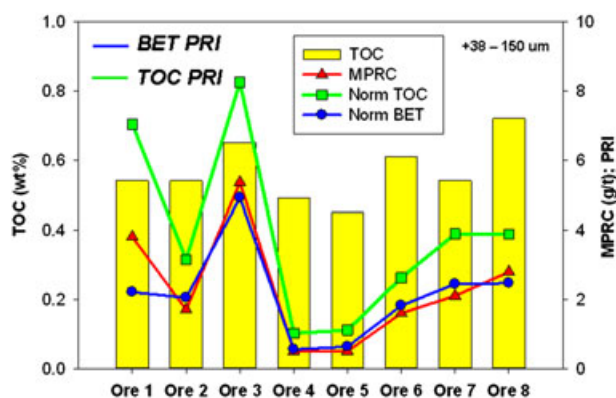

Figure 8. Total organic carbon (TOC) and maximum preg-robbing capacity (MPRC) for the +38–150 μm fraction from 8 ore samples within a single deposit. Also shown are the values for the MPRC normalized to the TOC and the BET surface area

information on the composition, size distribution, association, and liberation characteristics of the visible gold (native gold, electrum, and gold minerals) present in the sample.

The visible gold scan procedure involves initial back scatter electron (BSE) imaging to identify grains as possible candidates for gold/gold mineral phases followed by energy dispersive X-ray (EDX) spectroscopy verification of their composition. Following this procedure, gold-related (Au, Au + Ag, Au minerals), mineral particles are identified in the corresponding samples and further analyzed for their size distribution, liberation, and host association.

The analysis classifies the visible gold present in the sample into 4 different categories: free, attached, attached/locked, and (fully) locked (Figure 9). The attached/locked category applies to visible gold grains that are partially embedded in other minerals and have less exposed surface area for direct cyanide leaching. The first 3 categories represent the visible gold that is recoverable (or at least partially recoverable) by direct cyanidization.
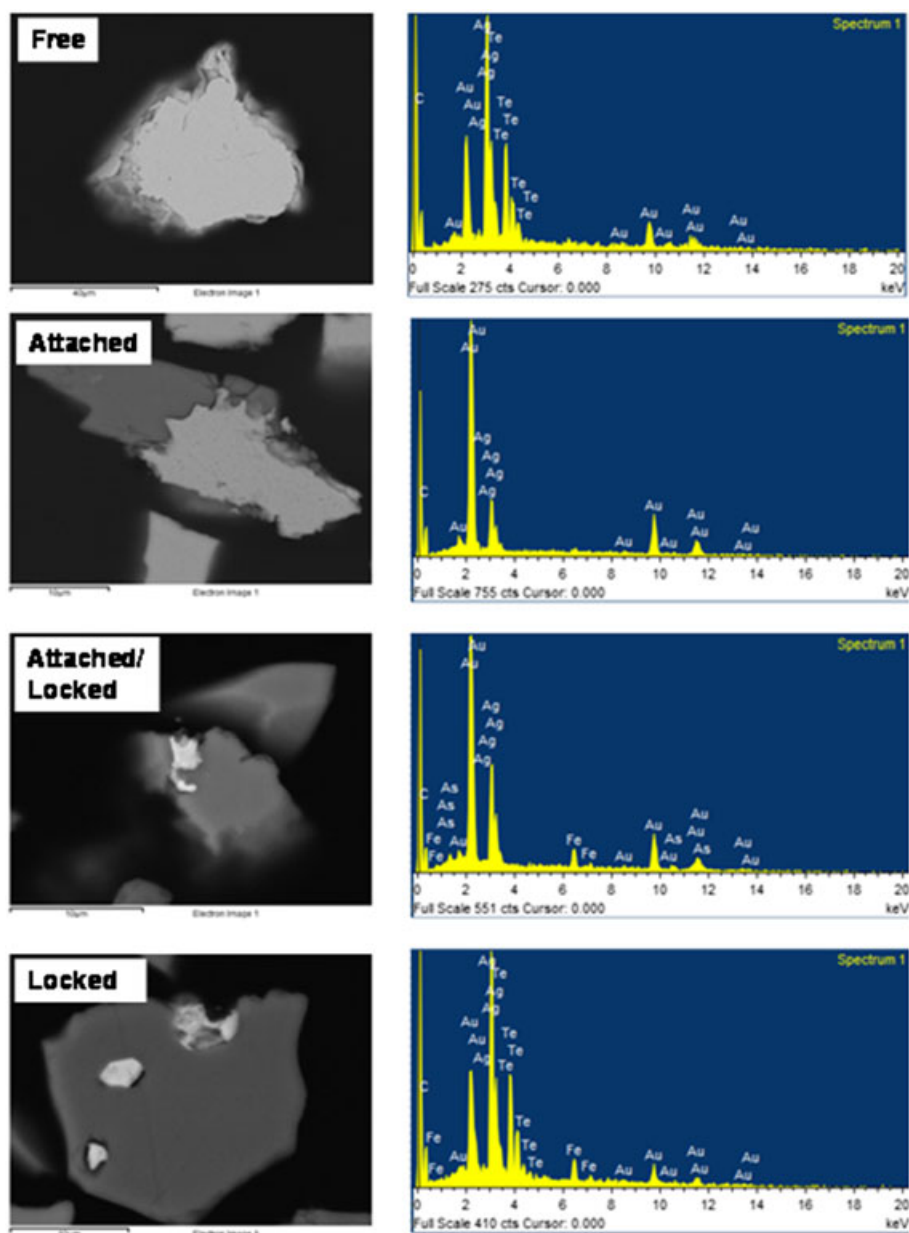
Figure 9. BSE images and EDX compositional spectra of visible gold grains associated with 4 different categories: free, attached, attached/locked, and locked visible gold grains

*Morphological classification of the visible gold in the sample:*

- *Classification based on size distribution*: The determined size distribution and liberation (free, attached, attached/locked, and locked) of gold particles, based on the number of particles identified in each class/sample.

- *Classification based on surface area:* Classification based on the total surface area determined for various classes (free, attached, attached/locked, and locked). This takes into account the different size distribution of gold particles in the samples and is a better measure for recoverable (free + attached + attached/locked) versus unrecoverable gold (locked) in each sample.

The example provided in Figure 10 shows significant differences between the cyanide feed sample (CILF) and the cyanide leached tails sample (CNLT) in the distribution and liberation of the visible gold. After the completion of the cyanide leaching process, the cyanide leach tail sample still contains some residual (unrecovered) visible gold. The data show that, for the CNLT sample, based on surface area data, only 6% of the visible gold contained is recoverable, while the remainder occurs as physically locked visible gold inclusions.

Visible gold leaching issues

It is possible that liberated visible gold grains do not fully dissolve during the cyanidation leaching process. Probable causes for poor leaching may be related to gold grain composition and/or the presence of surface coatings that inhibit the leaching process. Gold mineral phases containing Bi, Te, and Sb (for example maldonite, sylvanite, and calaverite) show refractory behavior under normal leaching conditions. Slower leaching kinetics for Ag, Hg, Bi, Te, or Sb present in the gold grains can lead to their enrichment and
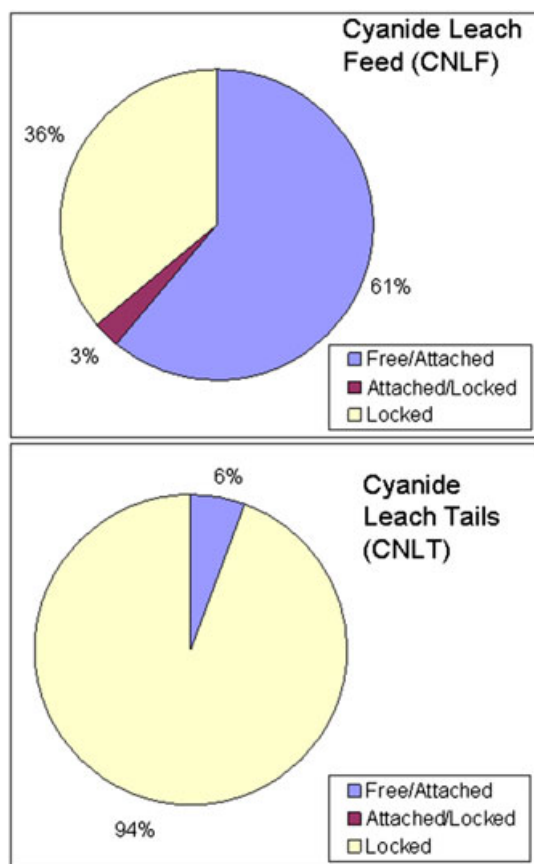
Figure 10. Gold grain surface area distribution within the cyanide leach feed and cyanide leach tails samples from the same process. The data show the relative surface area exposure of the liberated classified grains and illustrate that more than 90% of the total Au grain potentially available for leaching was recovered. Percentages are normalized to the total surface area of gold grains identified in each sample

leaching process (eg, organic collectors or iron hydroxides) can also inhibit the leaching of gold grains or minerals.
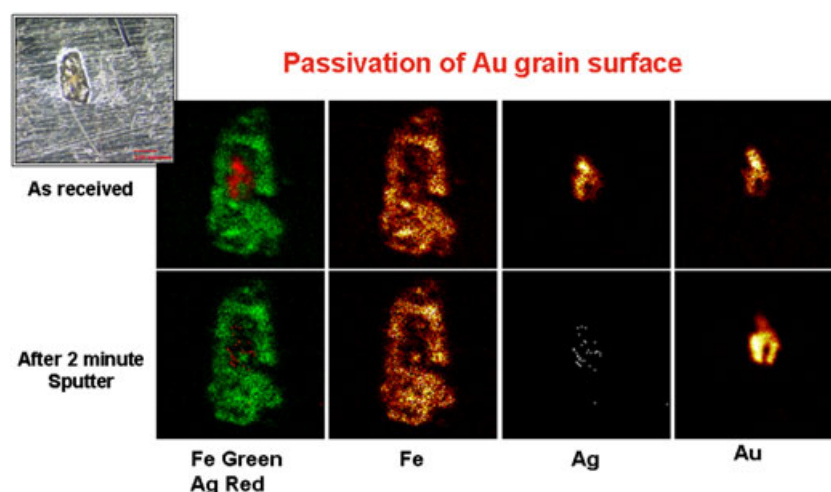
A comparative TOF-SIMS surface analysis on gold grains from leach feed samples and residual, unleached gold grains from the corresponding leach residue sample can provide valuable information on their surface composition and identify the presence of such passivating coatings on the unleached gold grains.

Example on surface coating on unleached gold grain from cyanide leach tail sample identified by TOF-SIMS analysis is shown in Figure 11.

Characterization of submicroscopic (refractory) gold

The dynamic SIMS is a benchmark technique for quantitative analysis of submicroscopic (invisible) gold and other precious metals in minerals.[2,3] The submicroscopic gold detected and quantified by the dynamic SIMS is refractory gold, ie, it is locked within the crystalline structure of the mineral phase (most often in sulfide minerals), and it cannot be directly released by the cyanide leach process. This type of gold may be present as finely disseminated colloidal size gold particles (<0.5 μm) or as a solid solution within the mineral matrix. Dynamic SIMS utilizes an energetic primary ion beam which sputters consecutive layers of material from the surface of polished mineral grains. Some of the sputtered particles are ejected as positive or negative ions which carry information about the composition of the sample and are further analyzed in a magnetic sector mass spectrometer. By rastering the primary ion beam across the surface of the polished mineral grain, it is possible to map the distribution of the submicroscopic gold present in the mineral. The superiority of this technique to any other microbeam technique used for characterization of submicroscopic gold is related to the following features;

i) Sensitivity: The detection limits for the technique are in the range of 0.2 ppm with imaging capabilities at a spatial resolution of 1 μm.

ii) Accuracy: The quantification of the D-SIMS data is based on mineral specific ion implanted standards which results in elimination of any mineral matrix effects. The use of such matrix matched standards results in calibration curves covering a large dynamic range from 0.2 ppm to several wt%.

build-up of a passivating surface coating on the gold grains which could impede the process of cyanide leaching. Furthermore, the presence of other surface coatings on the gold grains before the

Figure 11. TOF-SIMS ion maps for selected surface species detected on a gold grain from cyanide leach tails before (original "as received" surface) and after removing the upper surface layer by sputtering with a Cs$^+$ ion source. This gold grain was attached to a pyrite grain (green color map). The ion maps show an Ag coating on the surface of the gold grain
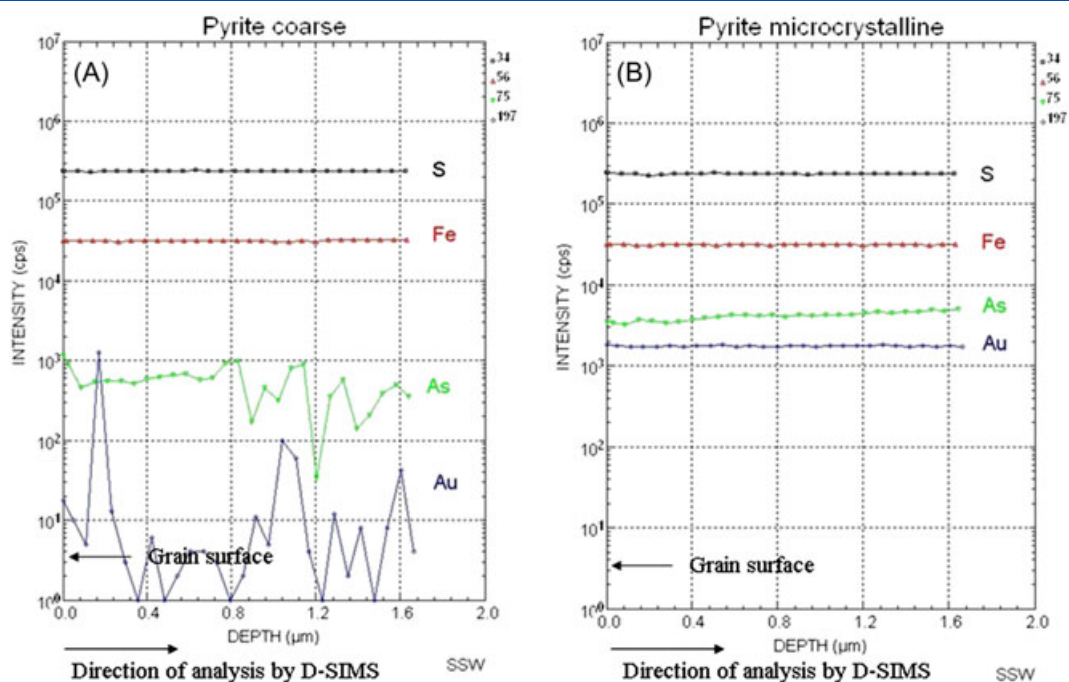
Figure 12. Dynamic SIMS depth profiles of submicroscopic gold in pyrite: (A) colloidal type submicroscopic gold in pyrite; (B) solid solution type submicroscopic gold in pyrite
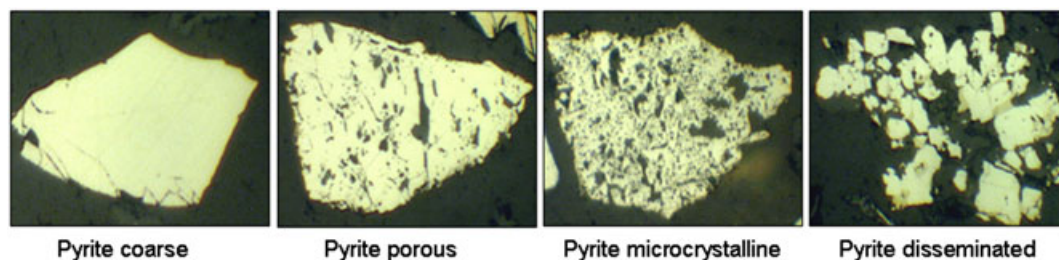

Figure 13. Morphological types of pyrite analyzed by the dynamic SIMS

iii) The D-SIMS data provide valuable information on the type of the submicroscopic gold in each carrier; solid solution gold or finely disseminated colloidal size (<0.5 μm) gold particles. Examples of D-SIMS depth profiles in pyrite grains (Figure 12) show the distribution of the basic matrix elements (S and Fe) as well as the trace elements, Au and As. The spikes in the gold signal intensity in the depth profiles represent colloidal type, submicroscopic gold (Figure 12A). The typical size is in the range of 100 to 200 nm. Dynamic SIMS depth profiles for solid solution, submicroscopic gold show a steady (flat) Au signal similar to the matrix elements, but with different levels of intensity depending on the concentration of submicroscopic gold present in the mineral (Figure 12B).

By analyzing a sufficient number of individual grains from each mineral phase of interest, it is possible to achieve a good statistical representation and an accurate quantitative estimate of the submicroscopic gold content in the various mineral carriers present in the sample.
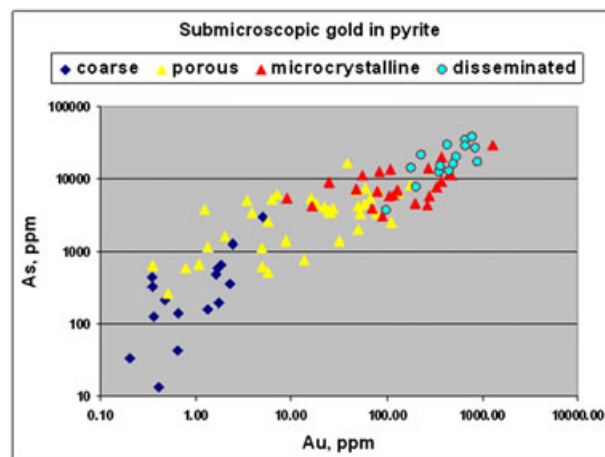
Figure 14. Scatter plot of gold and arsenic concentration in different morphological types of pyrite from flotation feed sample. Note: the Au and As concentrations are plotted logarithmically
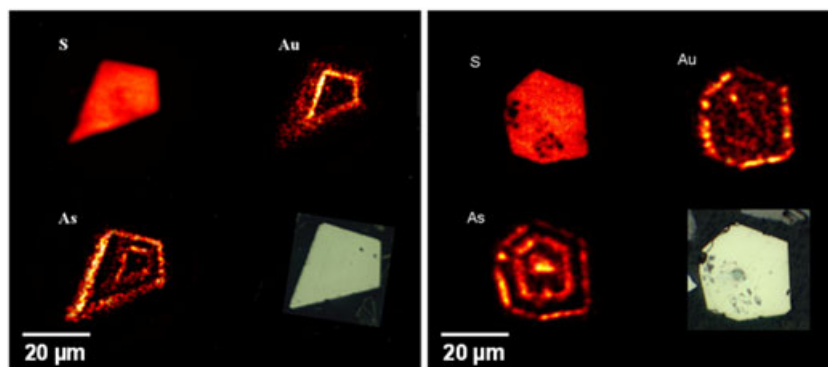
Figure 15. Images of distribution of submicroscopic gold and arsenic in pyrite mineral grains produced by dynamic SIMS. Also shown is a map for the matrix element S and an optical photograph of the grain
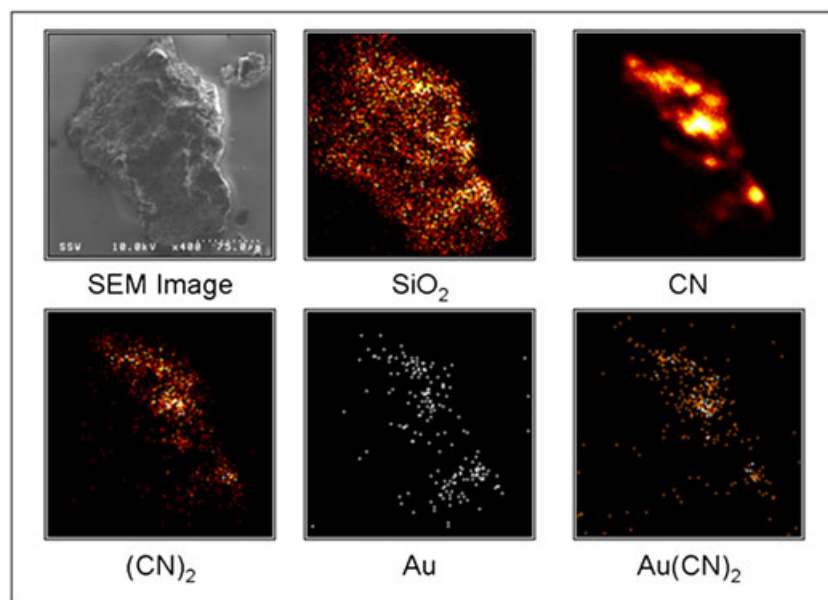
Figure 16. Optical image and TOF-SIMS elemental and compositional maps for carbonaceous particle from CIL tails sample. The quantified amount of metallic gold on this particle was 4.5 ppm, while the amount of Au as Au(CN)$_2$ compound gold was 38.1 ppm

Pyrite and arsenopyrite are common carriers of submicroscopic gold in refractory gold bearing ores. They are present as various morphological types with submicroscopic gold concentrations that can vary up to several orders of magnitude. The D-SIMS analysis can quantify the Au concentrations in the morphological sulfide types. This information is then compiled to provide gold balance estimates by taking into account the abundance of the morphological types and the determined corresponding average submicroscopic gold concentrations for each one of these types and/or carriers in the ore. Figure 13 shows several examples of various morphological types of pyrite. The correlations between Au/As content for these morphological types of pyrite in this particular ore are presented in Figure 14.

D-SIMS can also provide high resolution maps with distribution of trace elements at concentrations down in the low ppm range (Figure 15).

Characterization of surface gold preg-robbed on carbonaceous matter

The characterization of surface gold preg-robbed on C-matter is important for gold deportment studies in process stream products such as direct cyanidation tails or AC POX residues/CIL tails.

This procedure has 2 different objectives:

- Detection and speciation of different forms of gold preg-robbed on carbonaceous matter: metallic gold Au° and various gold compounds such as Au(CN)$_2^-$, AuCl$_2^-$, and AuS(CN)$_2^-$
- Quantification of the established forms of preg-robbed gold based on compound specific Au standards in activated carbon.

The characterization of the preg-robbed surface gold on C-matter is accomplished by TOF-SIMS.[2,5] This advanced surface
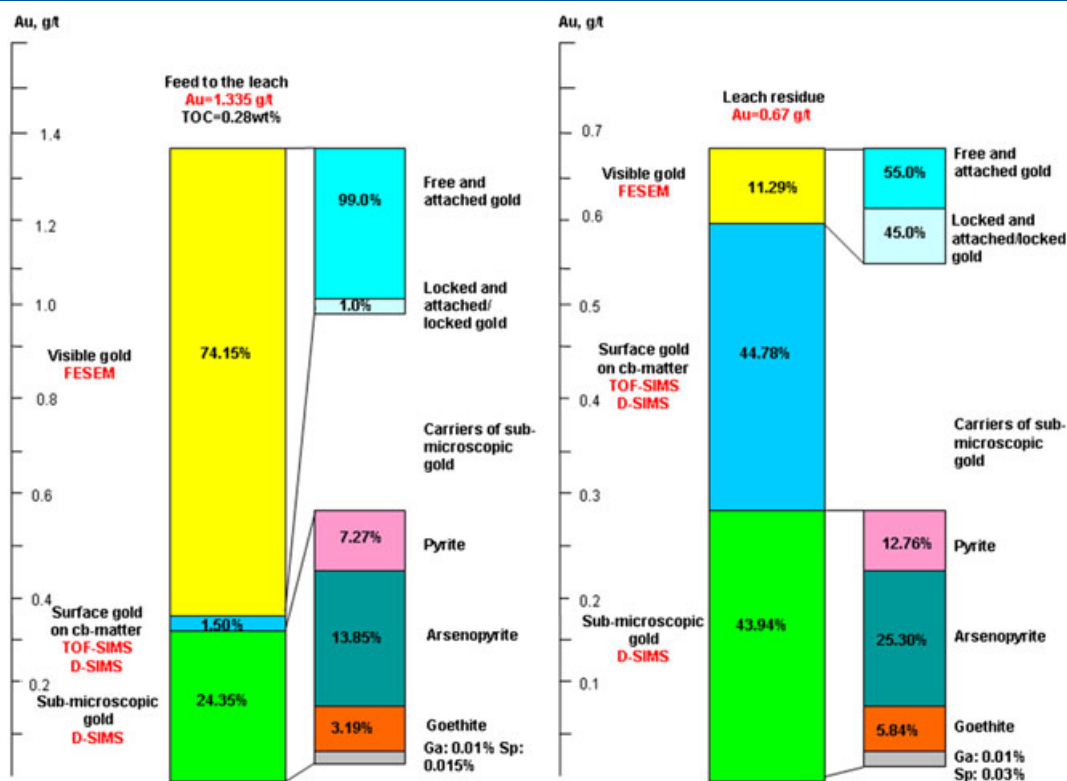
Figure 17. Gold deportment diagrams representing all major forms and carriers of gold in a cyanide feed and direct cyanidation leach residue samples. The relative distribution of gold per carrier is given in % of the total assayed value for gold in each sample. The corresponding techniques utilized for independent characterization/quantification of these forms of gold are identified on the diagrams

analytical technique provides nondestructive, organic, and inorganic surface analysis with detection sensitivity in the low ppm/ppb range. Due to the very low molecular fragmentation during the TOF-SIMS analysis, it is possible to detect ("speciate") simultaneously the presence of Au in both elemental (Au^0) and compound forms such as $Au(CN)_2$, $AuCl_2$, $Au(SCN)$, and $Au(SO_3)_2$. This information not only helps to balance the gold in these products but provides valuable insight into the chemistry and origin of gold losses during these processes. The quantification of the TOF-SIMS data is based on element and compound specific standards with established detection limits for surface metallic and compound gold in the low ppm range.

The TOF-SIMS analysis is carried out on individual, as received, carbonaceous particles and provides direct, independent determination of the surface gold present on these particles. By scanning the primary ion beam over the analyzed particle, it is possible to generate maps showing the surface concentration distribution of gold species across the particle. Example of TOF-SIMS images of surface gold species on a carbonaceous particle from a POX CIL residue sample is shown on Figure 16.

The D-SIMS technique can also be used for quantification of the total preg-robbed surface gold on carbonaceous matter. Due to the total fragmentation of all gold compounds during the D-SIMS analytical process, only Au ions will be detected, representing both the metallic and original compound gold species present on the surface of the C-matter. The quantification of the D-SIMS data is based on the use of external activated carbon standards. The D-SIMS offers better detection sensitivity for preg-robbed surface gold with detection limits in the ppb range.

Gold deportment diagrams

The gold deportment studies provide detailed gold mineral and metal deportment balances among samples and ore zones. Gold deportment diagrams are often used to provide visual representation of the distribution of the various forms and carriers of gold in samples from process stream products. An example of gold deportment diagrams on the established gold distribution in a cyanide feed sample before and after the gold recovery process is shown in Figure 17. The diagrams can provide insight into potential sources of Au loss in processing, establish where losses have occurred in process streams, and, potentially, identify opportunities for gold recovery improvement.

Conclusions

The implementation of advanced microbeam analytical techniques in gold deportment studies has greatly improved and expanded our capabilities to accurately characterize and quantify the forms of gold in individual carriers in a variety of process stream products.

One particular aspect of a deportment study related to gold losses during the recovery process is the effect of the naturally occurring carbonaceous matter in the ore. In some gold-bearing ores, it can have a strong detrimental effect on the gold recovery due to its capacity to competitively adsorb (preg-rob) solubilized gold. The analytical protocol, described here, outlining the full characterization of the c-matter in terms of preg-robbing properties has become a useful diagnostic and predictive tool for metallurgical operations.

Recovery improvements can only be identified once the sources of loss are clearly defined. For gold recovery operations, optimization requires establishing accurate, comprehensive gold deportment balances in the feed and various process stream products. The application of advanced microbeam analytical techniques as part of a comprehensive mineralogical and analytical investigation of a metallurgical application has proven fruitful toward identifying opportunities and strategies for process improvement.

References

[1] S. L. Chryssoulis, L. J. Cabri, *Trans. Instn. Min. Metall. C*, **1990**, *99*, 1–10.

[2] S.S. Dimov, B. R. Hart, in Proceedings of the 50th Annual Conference of Metallurgists of CIM, *World Gold Conference 2011* (Eds: G. Deschenes, R. Dimitrakopoulos, J. Bouvhard), Montreal, Canada, **2011**, pp. 17–26.

[3] S. S. Dimov, B. R. Hart, Santiago Chile, Chapter 1408, Geometallurgy and mineral processing, *IMPC*, **2014**, Oct, 20–14.

[4] S. S. Dimov, S. L. Chryssoulis, R. N. Sodhi, *Appl. Surf. Sci.*, **2003**, *203-204*, 644–647.

[5] S.S. Dimov, B. Hart, A. Chattopadhyay, in Proceedings of the 48th Annual Conference of Metallurgists (COM 2009) (Eds: C. Hamilton, R. Hart, P.J. Whittaker), Sudbury, Canada, **2009**, pp. 85–91.

[6] S. S. Dimov, S. L. Chryssoulis, in *Proceedings of the TMS Symposium: Analytical Technology in the Mining Industries* (Eds: L. J. Cabri, C. H. Bucknam, S. L. Chryssoulis), A publication of the Minerals, Metals and Materials Society, San Diego, USA, **1999**, pp. 209–219.

[7] B.R. Hart, S.S. Dimov, R. Mermillod-Blondin, J. Fournier, in Proceedings of the 50th Conference of Metallurgists of CIM, World Gold Conference 2011, Montreal Canada, **2011**, pp. 35–50.

[8] R. Dunne, W.P. Staunton and K. Afewu, World Gold Conference 2013, Brisbane QLD, **2013**, pp. 99–110.

[9] M. Helm, J. Vaughan, W.P. Staunton, J. Avraamides, World Gold Conference 2009, The Southern African Institute of Mining and Metallurgy, **2009**, pp.139–144.

[10] L.L. Coetzee, S.J. Theron, G.J. Martin, J.D. van der Merwe, T.A. Stanek, SGS Mineral Services, TP 2011–04.

[11] S. L. Chryssoulis, J. McMullen, in *Gold Ore Processing* (Ed: M. Adams) (2nd edn), **2016**, *15*, pp. 57–93.